Water Research 286 (2025) 124187

Contents lists available at ScienceDirect

Water Research

journal homepage: www.elsevier.com/locate/watres

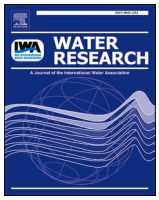

Identification of a surface protein in the extracellular polymeric substances of seawater-adapted aerobic granular sludge

Le Min Chen [a], Tessa Hofstra [a], Jelle Langedijk [a], Sebastian Andrei [a], Martin Pabst [a], Mario Pronk [a,b], Mark C.M. van Loosdrecht [a], Yuemei Lin [a,*]

[a] Department of Biotechnology, Delft University of Technology, Van der Maasweg 9, 2629 HZ Delft, the Netherlands
[b] Haskoning, Laan 1914 35, Amersfoort 3800 AL, the Netherlands

ARTICLE INFO

Keywords:
Extracellular polymeric substances
Aerobic granular sludge
Surface protein
Biofilm
Seawater

ABSTRACT

Identifying structural proteins within the extracellular polymeric substances (EPS) will provide a better understanding of the stability of aerobic granular sludge (AGS) and biofilms in general. In this work, an abundant surface protein was identified and localized in the extracellular matrix of seawater-adapted AGS. Granules with good phosphate removal were cultivated in a sequencing batch bubble column reactor with acetate as a carbon source dissolved in seawater. "*Candidatus* Accumulibacter" was observed as the most dominant community member through fluorescent *in-situ* hybridization. A surface protein of 74.5 kDa was identified in the EPS extract of the seawater-adapted AGS by SDS-PAGE and mass spectrometry. The surface protein was produced by an Accumulibacter species and showed homology to S-layer proteins. A type 1 secretion system was found adjacent to the gene encoding for the surface protein, suggesting a possible export system. Antibodies generated from a unique peptide of the surface protein confirmed the extracellular location of the surface protein. Microscopy observations with antibody staining showed the surface protein forms dense structures within the Accumulibacter microcolonies and larger fiber structures around the microcolonies. These observations highlight the importance of the protein for the structural properties of the granule. To detect more structural proteins in the EPS, optimization of the EPS extraction and *in situ* imaging validation methods are essential.

1. Introduction

With the increasing global shortage of freshwater, the use of seawater has become an attractive solution for various applications, including fire control, road and toilet flushing in coastal cities (Zhang et al., 2023a, 2023b). Moreover, industries such as leather-, food-processing, and pharmaceutical industries, may discharge saline wastewater due to the processing (Lefebvre and Moletta, 2006; Zhao et al., 2020a). The saline wastewater will be discharged into wastewater treatment plants for further treatment.

Among all the treatment processes, aerobic granular sludge (AGS) technology has emerged as a promising technology to treat saline wastewaters (Bassin et al., 2011; de Graaff et al., 2020a; Zhao et al., 2020b), thanks to its reduction in area usage, lower energy costs and potential for resource recovery (Pronk et al., 2015; Van Loosdrecht and Brdjanovic, 2014). In the AGS process, granules with microorganisms embedded in a self-produced matrix of extracellular polymeric substances (EPS) are formed. The EPS keeps the stability of the granules and protects the microorganisms from harsh environmental conditions, such as salinity in the form of seawater or NaCl (Decho and Gutierrez, 2017). The stabilizing mechanism of EPS is still unknown, which is largely due to the uncharacterized nature of the EPS matrix (Seviour et al., 2019).

The EPS is composed of various components, such as polysaccharides, extracellular enzymes, and structural proteins. These components interact together to form a matrix supporting microbial growth under dynamic and stressful environments (Flemming and Wingender, 2010). Studies on AGS adapting to saline conditions have shown an increase in EPS, protein content, and hydrophobicity at higher salinities (Campo et al., 2018; Corsino et al., 2017; Ou et al., 2018). Notably, proteins make up to 40 % of the extracted EPS and are found to play an important structural role in AGS stability (Felz et al., 2016; McSwain et al., 2005; Zhu et al., 2015). In addition, specific structural proteins have been linked to the stability of granular sludge. Amyloid

* Corresponding author.
E-mail address: Yuemei.Lin@tudelft.nl (Y. Lin).

https://doi.org/10.1016/j.watres.2025.124187
Received 15 April 2025; Received in revised form 19 June 2025; Accepted 7 July 2025
Available online 8 July 2025

proteins have been identified to play a structural role in AGS enriched with ammonia-oxidizing bacteria (Lin et al., 2018). Similarly, glycosylated S-layer proteins have been found to form a large fraction of the EPS in anammox granules acting as an adhesive and facilitating assembly with other community members (Boleij et al., 2018; Pabst et al., 2022; Wong et al., 2023). These reports highlight the importance of (structural) proteins in the EPS of granular sludge. However, no structural proteins have been identified in saline AGS to date.

Identification of EPS components involved in seawater AGS, especially (structural) proteins, will not only expand our database of important EPS components, but also allow a better understanding of the role that the EPS plays in maintaining the stability of AGS. Insight into EPS composition and their interactions within the extracellular matrix may reveal their functions. Understanding of these functions and how they are regulated could generate knowledge on a better control of AGS process. Additionally, this may also open new opportunities and/or strategies for recovering EPS as a sustainable resource (Seviour et al., 2019). Therefore, the goal of this work was to identify the extracellular protein(s) in seawater-adapted AGS, visualize its distribution *in situ,* and understand its potential role in the granule. To this end, the extracellular proteins were extracted from AGS and an abundant protein was identified using mass spectrometry. *In situ* immunostaining was performed to localize the dominant protein.

2. Material and methods

2.1. Reactor operation and microbial community analysis

2.1.1. Reactor operation

Aerobic granular sludge was cultivated in a 2.8 L bubble column (6.5 cm diameter) as a sequencing batch reactor (SBR) as adapted from (de Graaff et al., 2019). The seawater-adapted reactor was inoculated with 600 mL 1:1 vol ratio activated sludge from the wastewater treatment plant in Harnaschpolder The Netherlands and full-scale Nereda® sludge from Utrecht, The Netherlands. The temperature of the reactor was controlled by controlling the room temperature at 20 °C. The pH was controlled at pH 7.3 ± 0.1 by dosing either 1.0 M NaOH or 1.0 M HCl. The dissolved oxygen (DO) was controlled by a mixture of nitrogen gas and air at 0 % and 80 % (5.9 mg O_2/L in seawater) in the anaerobic and aerobic phases, respectively.

Reactor cycles consisted of 5 min settling, 5 min effluent withdrawal, 5 min N_2 sparging, 5 min of feeding, 50 min N_2 gas sparging (anaerobic phase), and 110 min of aeration (aerobic phase). The average sludge retention time (SRT) was kept at 13 ± 1 days by manual sludge removal for both reactors. Granules were samples for analysis at least 3 months of steady reactor performance in growth and phosphate removal for the first and second reactor, respectively.

The feed of 1.5 L per cycle consisted of 1.2 L artificial seawater (final concentration 30 g/L, Instant Ocean®), 150 mL of medium A and 150 mL of medium B. Medium A was composed of 62.5 mM of sodium acetate trihydrate. Medium B contained 41.13 mM of NH_4Cl, 0.34 mM of K_2HPO_4, 0.27 mM of KH_2PO_4, 0.07 mM of allylthiourea and 10 mL/L of trace elements solution similar to Vishniac & Santer (1957), but using 2.2 g/L of $ZnSO_4{\cdot}7H_2O$ instead of 22 g/L and 2.18 g/L of $Na_2MoO_4{\cdot}2H_2O$ instead of $(NH_4)_6Mo_7O_{24}{\cdot}4H_2O$. The combination of these feed streams led to influent concentrations of 400 mg/L COD, 50 mg/L NH_4—N, and 12.2 mg/L PO_4-P. To monitor the performance of the reactor, samples were taken at certain intervals and filtered through a 0.22 μm PVDF filter. Acetate concentration was measured through high-performance liquid chromatography, HPLC, (Thermo Scientific Vanquish HPLC) at 50 °C (0.75 mL/min) with 1.5 mM phosphoric acid as eluent and Aminex HPC-87H (Bio-Rad, California, USA) as a column. Phosphate and ammonia concentrations were measured using a Thermo Fisher Gallery Discrete Analyzer (Thermos Fisher Scientific, Waltham, USA).

The organic and ash fractions of the biomass were determined according to the standard methods (APHA, 1998). Pictures of the granules were taken with a stereo zoom microscope (M205 FA, Leica Microsystems, Germany) connected to the Eert Vision Auto Focus Microscope camera (Eert Vision, The Netherlands), and the images were acquired with the Eert C304 software (V1.0, Eert Vision, The Netherlands). For protein extraction, the granules were rinsed with demi water to remove excess salt, lyophilized immediately, and stored at room temperature.

2.1.2. Microbial community analysis by fluorescent in-situ hybridization (FISH)

The granules were collected from the reactor at the end of the aerobic phase. The handling, fixation and staining of FISH samples were performed as described in Bassin et al., 2011. The PAO651 probe was used for visualizing the polyphosphate accumulating organism (PAO), "*Candidatus* Accumulibacter" (Albertsen et al., 2016). The GAOmix (GAOQ431 and GAOQ989) was used for visualizing glycogen accumulating organisms (GAO) (Crocetti et al., 2000). EUBmix (EUB338, EUB338-II and EUB338- III) were used for staining all bacteria (Amann et al., 1990; Daims et al., 1999). Images were taken with a Zeiss Axio Imager M2 microscope equipped with the fluorescent light source X-Cite Xylis 720 L. The image acquisition was performed with the Zeiss Axiocam 705 mono camera. The images were processed and exported in .tif format with the Zeiss microscopy software (ZEN version 3.3).

2.2. Isolation and identification of the abundant EPS proteins

2.2.1. Protein extraction and gel-electrophoresis

Optimization of the extraction method was first performed by varying the type of biomass (wet pellet, lyophilized granules), the concentration of lyophilized granules (3.2 – 12.8 mg/mL), temperature (5, 20, 60 and 80 °C), chemical (NaCl, Na_2CO_3) and time (1, 6, and 24 h) while assessing the intact protein bands on the SDS-PAGE. The optimal extraction condition was considered if the extraction method yielded the strongest protein bands on the SDS-PAGE. The optimal extraction method was found as follows: lyophilized granules of the seawater-adapted reactor were crushed and extracted using0.5 % w/v Na_2CO_3 (Felz et al., 2016) at a concentration of 12.8 mg lyophilized biomass / mL. The extraction was performed overnight (approx. 15 h) while stirring at 400 rpm at room temperature (20 °C). After the extraction, the pellet was discarded by centrifuging at 14.000 × *g* for 5 min at 5 °C. The extracted proteins in the supernatant were denatured in dithiothreitol (12.5 mM) and NuPAGE LDS Sample Buffer 4x (Thermofischer Scientific) at 70 °C for 10 min. 10 μL of each sample was loaded on the NuPage ® Novex 4–12 % Bis-Tris gels (Invitrogen). The Multicolor Broad Range Protein ladder (Thermofischer Scientific) was used as a molecular weight marker. The electrophoresis was performed for 35 min at 200 V in NuPAGE MES SDS running buffer (Thermofischer Scientific). The gel was stained by either Coomassie Blue (Simply Blue, Invitrogen) or PAS staining (Pierce Glycoprotein Staining Kit), both following the manufacturer's instructions. The gels were visualized on a ChemiDoc MP Imaging System (Bio-Rad, Hercules, *CA*).

2.2.2. In-gel digestion

Sample preparation and proteomics analysis of SDS-PAGE separated samples were performed as described in Pabst et al. (2022) SDS-PAGE analysis and in-gel digestion. To extract the peptides from the gel, the gel band was first cut out from the Coomassie-stained gel into smaller pieces and destained in destaining solution (100 mM NH_4HCO_3 in 40 % acetonitrile, ACN) for 15 min at room temperature. The destained gel pieces were incubated in the following solutions step-by-step as follows: 1) 200 μL 100 % ACN for 10 min at room temperature for dehydration. 2) 200 μL 10 mM DTT in 100 mM NH_4HCO_3 for 30 min at 56 °C at 300 rpm for reduction of the cysteine residues. 3) Alkylation of the cysteine residues was performed by adding 200 μL of freshly prepared 55 mM iodoacetamide in 100 mM NH_4HCO_3 for 30 min at room temperature in the dark. The alkylation solution was replaced by destaining solution for 5 min at room temperature. The gel pieces were dehydrated again as

described above. The dehydrated gel pieces were rehydrated in 98 μL of 100 mM NH_4HCO_3 and 2 μL digestion solution (Trypsin Sequencing Grade, Promega, 0.1 μg/μL in 1 mM HCl in LC-MS H_2O). The sample was digested overnight (approx. 18 h) at 37 °C and 300 rpm. After the digestion, the solution was collected. The in-gel peptides were further extracted using 150 μL of peptide extraction solution (70 % ACN with 5 % formic acid, FA, in water) for 15 min at 37 °C, collecting the solution. Then another extraction was followed using 100 μL solution of 10:90 ACN:water for incubated for 15 min at 37 °C and collected. The extracted sample (approx. 450 μL) was subsequently dried in the SpeedVac concentrator (SPD1010–230, Thermo Scientific) at 45 °C for approximately 2 h. Finally, the sample was re-dissolved in 20 μL 3 % ACN, 0.1 % FA in H_2O prior to injection into the mass spectrometer.

2.2.3. Shotgun proteomics and data processing

The purified peptides were analyzed using a Q Exactive plus Hybrid Quadrupole-Orbitrap Mass Spectrometer (Thermo Scientific, Germany) connected online to an EASY-nLC 1200 system (Thermo Scientific, Germany). Chromatographic separation employed an Acclaim PepMap RSLC RP C18 separation column (50 μm x 150 mm, 2 μm) with solvents A (1 % ACN, 0.1 % FA) and B (80 % ACN, 0.1 % FA). A gradient from 5 % to 35 % B over 88 min, followed by a linear gradient up to 65 % B over another 30 min, was maintained at a constant flow rate of 350 nL/min. Approximately 4 μL of the proteolytic digest each was injected. Electrospray ionization was performed in positive ionization mode, and MS1 analysis was executed at a resolution of 70 K, with an AGC target of 3.0E6 and a maximum IT of 75 ms. The top 10 signals were selected for fragmentation, using an isolation window of 2.5 m/z. HCD fragmentation was performed using an NCE of 28. For MS2 analysis, a resolution of 17.5 K, an AGC target of 2.0E5, and a maximum IT of 100 ms were employed.

Mass spectrometric raw data were database searched using PEAKS X (Bioinformatics Solutions Inc., Canada) and a database constructed from whole metagenome sequencing experiments of a "*Ca.* Accumulibacter" enrichment (Kleikamp et al., 2021), complemented with Candidatus Accumulibacter sequences obtained from UniprotKB, allowing for a 20 ppm parent ion and 0.02 m/z fragment ion mass error, 3 missed cleavages, carbamidomethylation as fixed and methionine oxidation and N/Q deamidation as variable modifications. Peptide spectrum matches were filtered for 1 % false discovery rate and protein identifications with ≥ 2 unique peptides were considered significant. Analysis for the glycosylation was performed as described recently (Pabst et al., 2022).

2.2.4. Homology search

The obtained protein sequence was identified using the BLAST tool on NCBI and Uniprot using the standard parameters. The protein query was searched against the non-redundant protein sequences (nr) database and UniprotKB reference proteomes + Swiss-Prot, for NCBI and Uniprot, respectively. The identified protein (WP_313,950,548.1) was found in the CDS region (NZ_JAVTWB010000028.1) in the genome assembly ASM3222952v1.

2.3. In situ visualization of the identified extracellular protein

2.3.1. Antibody generation

The selected two unique peptides (GDK and AVA, Supplementary material) of the identified protein was generated and immunized on rabbits by David's Biotechnology (Regenburg, Germany). The immunization schedule protocol followed 5 immunizations (Day 1, 14, 28, 42 and 56), where on Day 35 a test bleed was performed to monitor antibody titer development. The final bleed was performed on Day 63. Affinity purification was performed to obtain a specific polyclonal antibody fraction at a concentration of 0.68 mg/mL and 0.95 mg/mL, respectively.

2.3.2. Immunoblotting

To determine the antibody specificity the purified antibody fraction was subjected to Western Blotting. After gel electrophoresis as described in section 2.2.1, the gel was transferred onto the Trans-Blot Turbo Mini PVDF membranes with a pore size of 0.2 μm (Bio-Rad, Hercules, *CA*). The proteins were transferred to the membrane at 25 V for 15 min at room temperature using the Trans-Blot® Turbo Transfer system (Bio-Rad, Hercules, *CA*).

After blotting, 100 ng of the generated peptides were added on the membrane as a positive control. The blot was cut into strips and blocked at room temperature for 1 hour in blocking buffer consisting of 5 % (w/v) skim milk powder in TBS-T (Tris 20 mM, NaCl 150 mM, pH 7.6, 0.1 % (w/v) Tween-20). The membrane strips were washed in 5 mL TBS-T three times for 5 min. The primary antibody was diluted to 0.01 mg/mL in TBS-T and from there the optimal dilution of 1:500 (final concentration 20 ng/μL) was used to incubate the membrane overnight at 4 °C. The optimal concentrations of primary antibody was determined by blotting using sequential concentrations of the primary antibody (1:500 – 1:15.000) and evaluating the blot intensity. The membrane was washed in six times 5 mL TBS-T for 5 min and incubated with 10.000-fold diluted Goat Ant-Rabbit IgG conjugated to horse radish peroxide (HRP) in TBS-T (final concentration 80 ng/mL) for 1 hour at room temperature. The membrane strips were washed in 5 mL TBS-T three times for 5 min. Afterwards, they were treated with 1 mL of HRP substrate (Immobilon® Crescendo Western HRP Substrate, Sigma-Aldrich) and visualized by chemiluminescence on the ChemiDoc MP Imaging System (Bio-Rad, Hercules, *CA*). Only one peptide was shown to be specific for the target protein, thus this was used for the subsequent immunostaining analysis. To confirm unspecific binding of the secondary antibody, a control was performed omitting the primary antibody (Supplementary material)

2.3.3. Granule slicing

Detailed methodology of granule slicing can be found Langedijk et al. (in preparation). Paraformaldehyde fixated granules were embedded in 5 % (w/v) agarose dissolved in demi water. The sample was attached to the vibratome (700smz-2 Vibratome, Campden Instruments, England) using cyanoacrylate glue and covered with seawater (Instant Ocean 30 g/L). The granule was cut into 10 μm slices at 0.5 mm/s and 50 Hz with a ceramic blade (Campden Instruments, England). The slices were collected on an Epredia™ SuperFrost™ Plus adhesion slides (Thermo Fisher Scientific, Waltham, MA) and dried to immobilize the slice to the slide.

2.3.4. Immunostaining

To visualize the surface protein, immunostaining was performed on sliced and pottered granules. The slides with either the slices or pottered granules were dehydrated sequentially in 50 %, 80 %, and 96 % (v/v) ethanol for 3 min each and air-dried. The immunostaining was followed similar to Wong et al. (2023). The optimal concentration of primary antibody (1:680) was determined after performing the immunostaining with different conditions. 5 % BSA was used due to the autofluorescence signal of the milk proteins in the same wavelength as the secondary antibody probe.

The slide was blocked overnight in a blocking buffer (5 % w/v BSA in TBS-T) at 4 °C with gentle shaking. The primary antibody was diluted to 1 μg/mL (1:680) in blocking buffer, 1 mL was added to cover the entire slide, and incubated for 1.5 h at room temperature with gentle shaking. The slide was washed in 20 mL of TBS-T three times for 5 min and air-dried. The secondary antibody, goat anti-rabbit IgG ($H + L$) – AlexaFluor488 (Thermo Fischer Scientific, Waltham, MA), was diluted 1:500 (final concentration 4 μg/mL) in blocking buffer and 250 μL was added on top of the slices and incubated for 1 h in a humidity chamber at room temperature in the dark. The slide was washed in 20 mL of TBS-T three times for 5 min and air-dried, followed by fixation with 4 % paraformaldehyde for 10 min at room temperature. The fixed slide was

rinsed with PBS followed by demi-water to remove the excess paraformaldehyde and salts. The fixed slide was dehydrated sequentially in 50 %, 80 %, and 96 % (v/v) ethanol for 3 min each and air-dried followed by the FISH protocol as described in section 2.1.2, omitting the fluorescein (498/517 ex/em) probe. As a negative control, the primary antibody was omitted (Supplementary material). Images were taken with a Zeiss Axio Imager M2 microscope equipped with the fluorescent light source X-Cite Xylis 720 L. The image acquisition was performed with the Zeiss Axiocam 705 mono camera. The images were processed and exported in .tif format with the Zeiss microscopy software (ZEN version 3.3).

3. Results

3.1. Reactor operation and microbial community analysis by fluorescent in situ hybridization (FISH)

The seawater-adapted AGS reactor showed good granule formation and enhanced phosphate removal performance. The granules had a size range of 0.5 – 3 mm in diameter (Fig. 1A). The phosphate release and acetate uptake during a typical cycle corresponded to a P:C ratio of 0.40 P-mol / C-mol. Similar ratios were observed in other AGS studies with a dominant population of the phosphate accumulating organism (PAO) "*Candidatus* Accumulibacter" ("*Ca.* Accumulibacter") (de Graaff et al., 2019; Weissbrodt et al., 2014; Welles et al., 2015). FISH analysis revealed a dominance of PAO "*Candidatus* Accumulibacter" in the microbial community, whereas glycogen accumulating organisms (GAO) were observed in small quantities, <10 % of the community (Fig. 1B). Only trace amounts of other bacteria (positive stain for general eubacteria probe EUBmix) were observed (Supplementary material). Overall, this shows that the microbial community in seawater-adapted AGS was dominant with "*Ca.* Accumulibacter.".

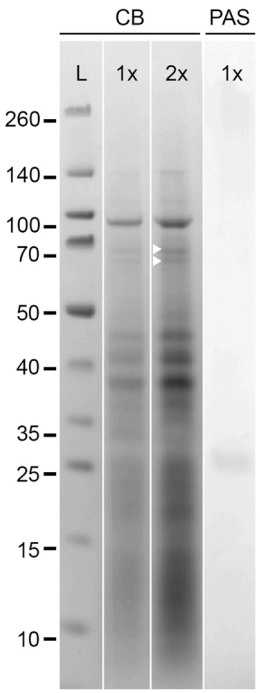

Fig. 2. SDS-PAGE of proteins extracted from seawater-adapted granules. L: ladder 1x: granules concentration at 6.4 mg/mL and 2x: granules concentration at 12.8 mg/mL CB: Coomassie blue staining for all proteins (L, lane 1x, 2x). PAS: Periodic acid staining for glycoproteins. Left of the ladder are the molecular weights indicated as kDa. The small white arrows at the lane 2x indicate the two weakly stained bands at around 70 kDa.

3.2. Identification of an abundant putative surface protein in seawater-adapted AGS

The proteins from the seawater AGS were extracted overnight in Na_2CO_3 and characterized using SDS-PAGE. Following Coomassie Blue staining, a strong band was observed at an apparent molecular weight of 100 kDa (Fig. 2, lane 1x), suggesting the presence of an abundant protein in the extract. This band was negatively stained by PAS (Fig. 2), indicating it is not glycosylated. Right under this band, two weakly stained bands were shown at around 70 kDa (when a higher concentration of biomass was used in the extraction, these two bands were more apparent, Fig. 2, lane 2x arrows). Furthermore, a range of smaller proteins was seen at the molecular weight lower than 50 kDa. Because the 100 kDa band was sharp and strong, it was taken as an indication that this protein is abundant in the granule. To further identify this protein, the Coomassie blue stained band was cut from the gel and digested into peptides for subsequent mass spectrometry analysis.

3.3. Proteomic analysis revealed the presence of a surface protein

The protein observed at 100 kDa in the electrophoresis gel was identified by mass spectrometry as a protein containing of 756 amino acids (full protein sequence is found in the Supplementary material). 44.7 % of the amino acids are hydrophobic of which alanine (17.7 %) is found in the highest abundance. 35.2 % of the amino acids are polar uncharged of which threonine (19.3 %) is found in the highest abundance. The charged amino acids make up 9.8 % of the total sequence. Notably, cysteine was not present in the protein sequence. The theoretical pI/Mw of this protein is 4.30 / 74.493 kDa according to the

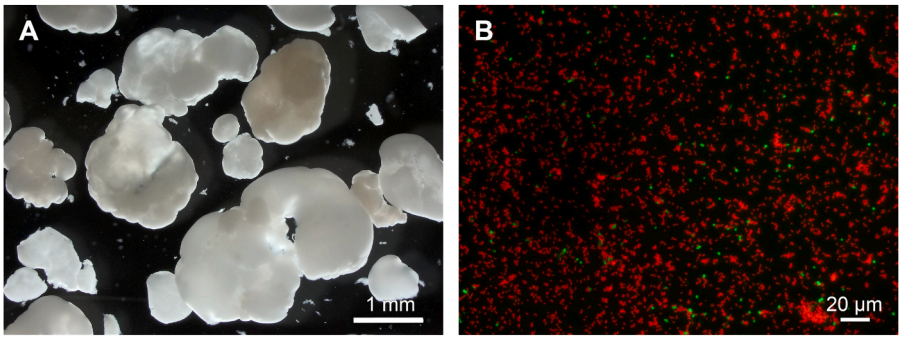

Fig. 1. Stereozoom pictures of aerobic granular sludge grown under seawater conditions (A). Fluorescent in-situ hybridization (FISH) PAO651 in red and GAOmix in green of disintegrated seawater granular sludge (B).

Table 1
BLASTp search of the surface protein in NCBI and Uniprot showing the hit (1) and the homology (2 - 4) of the putative surface protein with other proteins. The full BLASTp results from NCBI and Uniprot are found in the Supplemental material. Lower E-value indicates higher confidence that the similarity is not found by chance. E-values < 1E-25 indicate clear homology (Pearson, 2013).

	Description	Organism	E-value	%ID	Accession / Entry	Database
1	bluetail domain-containing putative **surface protein**	Accumulibacter sp.	0	100%	WP_313,950,548.1	NCBI
2	**beta strand repeat-containing** protein	Rhizobium oryzicola	7.00E-133	47.1%	WP_302,078,835.1	NCBI
3	**Calcium-binding** protein	Methylobacterium sp. Leaf99	1.80E-90	43.8%	A0A0Q4XER2	Uniprot
4	**S-layer protein rsaA**	*Caulobacter crescentus*	1.80E-41	30.5%	P35828	Uniprot

calculation by ExPASy.

Interestingly, when the full protein sequence was used as a query and BLAST against NCBI database, an exact sequence match was found to be a putative surface protein belonging to an unclassified Accumulibacter species (Table 1). Importantly, the conserved protein domain revealed that most of the amino acids (166–753) of this protein are arranged as β-sheets (with repeating β-strands), which has high similarity with the typical property of S-layer proteins (Bharat et al., 2017). Looking at the annotated proteins of other matches (2, 3 and 4 in Table 1), the E-value shows a good sequence homology, despite the low sequence identity. For the two proteins: beta strand-repeat containing protein and calcium-binding protein, they showed a match of 47.1 % and 43.8 % and E-values of 7E-133 and 1.8E-90, respectively. For the well-studied S-layer protein rsaA of *Caulobacter crescentus*, the match with our protein is only 30.5 %, while the E-value is low (1.8E-41). This suggests that the identified protein may be involved in calcium binding and/or is similar to surface layer protein (S-layer protein).

To further understand the putative function of the surface protein, the protein domains were evaluated through InterPro, and its structure was predicted by AlphaFold3. A C-terminal parallel β-roll was found consisting of two RTX repeats and 13 β-sheets (Fig. 3A). The parallel β roll structure is suggested to play a role in conformational arrangements upon binding with Ca^{2+}extracellularly (Guo et al., 2019), matching with the homologs annotated with Ca^{2+} binding property found above. The protein structure was found to consist of 35.2 % β-sheets and 18.8 % α-helix (Fig. 3B). At the N-terminal, 8 α-helix structures were found. Furthermore, the anchoring domain suggests that the protein may be anchored to the cell surface, thus the protein should be exported to the exterior by an export mechanism.

The protein was found to have four nonapeptide / RTX repeats, GGxGxDxUx, in the sequence (Fig. 3A), which is commonly found in proteins exported by the type 1 secretion system (T1SS) (Spitz et al., 2019). No export signal peptide was detected while using SignalP 6.0 (Teufel et al., 2022). To determine whether Accumulibacter sp. carries the genes encoding for T1SS, the genome protein sequence match was first identified. The exact sequence match was found present in the metagenome-assembled genome (MAG) of the Accumulibacter sp. from a lab-scale reactor fed with glucose (Elahinik et al., 2023) and preliminary search of seawater AGS metagenomics dataset of this study revealed the presence of the surface protein as well (Chen et al., in preparation). Four genes encoding for T1SS, together with the gene encoding for the surface protein, were found (Fig. 3C); two genes were annotated as T1SS permease / ATPase, one gene for HlyD the membrane fusion protein, and TolC the outer membrane protein, making up the complete T1SS (Kim et al., 2016; Spitz et al., 2019). Overall, the abundant protein in the seawater-adapted AGS is a surface protein, likely exported extracellularly by T1SS, and may be involved in a structural role similar to S-layer proteins.

To conduct *in situ* visualization of the protein in the granules, immunostaining was applied. The specificity of the generated antibody was validated by immunoblotting (Fig. 4). As expected, the antibody bound specifically to the protein at approximately 100 kDa, which is the same molecular weight as the band observed before with the Coomassie gel

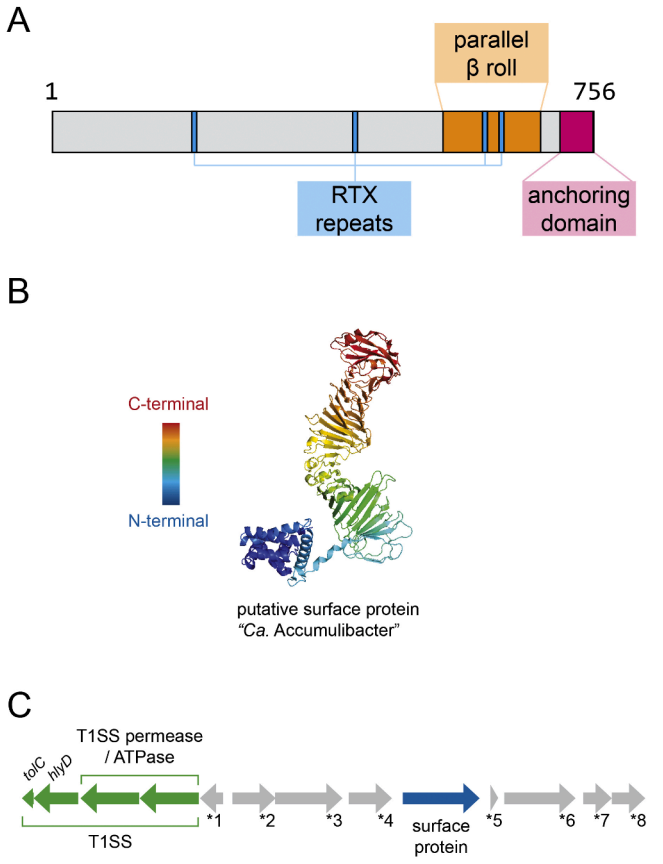

Fig. 3. Proteomic analysis of the surface protein. A) The secondary structure showing the parallel beta roll (IPR011049) and the surface-anchoring domain (IPR048165) towards the C-terminal of the protein predicted by InterPro and the RTX repeats (IPR001343). B) The 3D protein structure predicted by AlphaFold3. The prediction template modelling score (pTM) was 0.81, indicating a high-quality prediction (Abramson et al., 2024). The blue to red gradient indicates the N-terminal to the C-terminal of the protein respectively. C) Annotated genes around the gene encoding for the surface protein in the coding sequence region (CDS). Type 1 secretion system (T1SS) (in green) consisting of the outer membrane protein TolC, membrane fusion protein HlyD, and the ABC transporters T1SS permease / ATPase. Other annotated proteins: *1, hypothetical protein. *2, FecR family protein. *3, adenylate/guanylate cyclase domain-containing protein. *4, hypothetical protein. *5, DUF6447 family protein. *6, methyltransferase type 11. *7 ABC transporter permease. *8, ABC transporter ATP-binding protein.

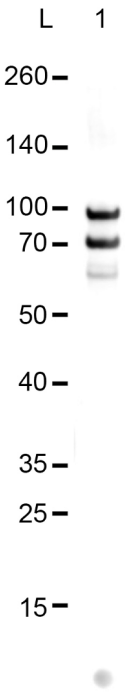

Fig. 4. Immunoblot analysis of the antibody generated against the unique peptide of the surface protein. The ladder (L) in kDa and the 6.8 mg/mL Na_2CO_3 extract from seawater (lane 1). A dot blot is presented on the bottom of the membrane of 100 ng of the unique peptide as a positive control.

(Fig. 2) The other bands that were present in the lower molecular weight range (< 45 kDa) with the Coomassie gel did not show any binding, indicating that the antibody is highly specific to the surface protein. Besides the 100 kDa band, the antibody was also found to interact strongly with a band at around 70 kDa, representing closely the theoretical molecular weight of 74 kDa. Although, shifts in apparent molecular weight can be caused by glycosylation (Scheller et al., 2021), the absent sugar staining and lack of glycosylation detected by the untargeted mass spectrometry approach suggest that the observed shift may instead result from different protein configurations, such as oligomerization and folding (Dunker and Rueckert, 1969).

3.4. Surface protein is found on the cell and in the extracellular matrix of seawater-adapted AGS

To visualize the location of the protein in the biomass, pottered biomass was used first. The antibody bound to the cell surface, showing a clear border around the rod-shaped bacteria (Fig. 5). Judging from the shape and the FISH analysis before, this organism resembles "*Ca.* Accumulibacter". The antibody was confirmed to have specific binding, as other bacteria, *e.g.* larger cocci shaped likely resembling GAO (Fig. 5A, B arrow), did not show any signal. Notably, about 1 μm long fibril-like structures were observed attached to the cells and in between the spaces of the cells (Fig. 5), suggesting that the surface protein could be part of the extracellular matrix of the seawater-adapted AGS.

Granule slices were used to visualize the distribution of the surface protein in the granules (Fig. 6). The surface protein was found to be distributed throughout the entire granule at different scales; around the microorganisms, within the microcolony, and in between the microcolonies. The surface protein was found around the "*Ca.* Accumulibacter" cells towards the loosely packed center of the granule (Fig. 6C), confirming the previous proteomic analysis and staining on pottered biomass. The areas in between the cells were also stained, similar to a web-like structure (Fig. 6C arrows). At the outer edge of the granule, the intensity of the surface protein signal was higher compared to the center (Fig. 6A, B, D). The individual cells within the microcolony appeared densely packed with the surface protein forming a compact honeycomb-like structure surrounding the cells and filling the spaces between them (Fig. 6B). This structure was consistently found across multiple granules. Lastly, a less common structure resembling large fiber strands with lengths >20 μm was also observed in between the microcolonies (Fig. 6E, F). The fibrous strands seemed to be present in the grooves of the granule where less "*Ca.* Accumulibacter" was observed (indicated by the lack of overlap of the signals). To summarize, it was observed that the surface protein was located in the microcolonies, as well as in the extracellular matrix of the granules. Within the microcolonies, this protein was found around the outer membrane and in the space between the cells. It built up a dense honeycomb structure filling in the microcolony, while large fibers were located in between the microcolonies.

4. Discussion

4.1. An abundant surface protein in seawater-adapted AGS has similarities with previously identified S-layer RTX protein

Identifying the components in the EPS is important to understand the stability of aerobic granular sludge or biofilms in general. In the current study, an abundant protein in the seawater-adapted AGS enriched with "*Ca.* Accumulibacter" was isolated and analyzed. It was revealed that this protein is a putative surface protein of Accumulibacter species. Especially, there are similarities with S-layer proteins. There is a low sequence similarity (30.5 %) and a low E-value (1.80E-41) of the identified protein to the well-characterized S-layer protein of *Caulobater crescentus* (Pearson, 2013). However, low homology is generally found

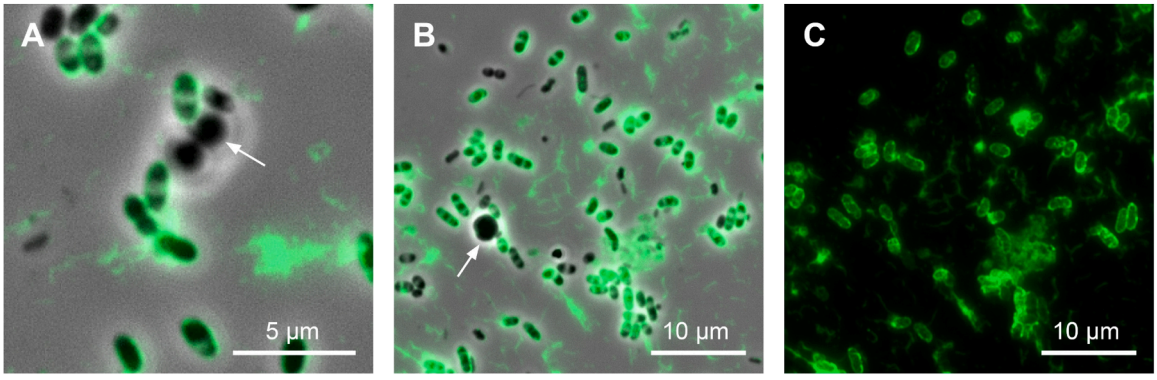

Fig. 5. Immunofluorescence staining of pottered biomass of seawater AGS (A, B, C). The white arrows (A, B) indicate the GAO. Fluorescence staining of AlexaFluor-488 was overlayed with phase contrast pictures (A and B) and only the fluorescence staining is shown for C. The exposure of AlexFluor-488 was kept the same across all pictures, allowing comparison of the signal intensity between samples.

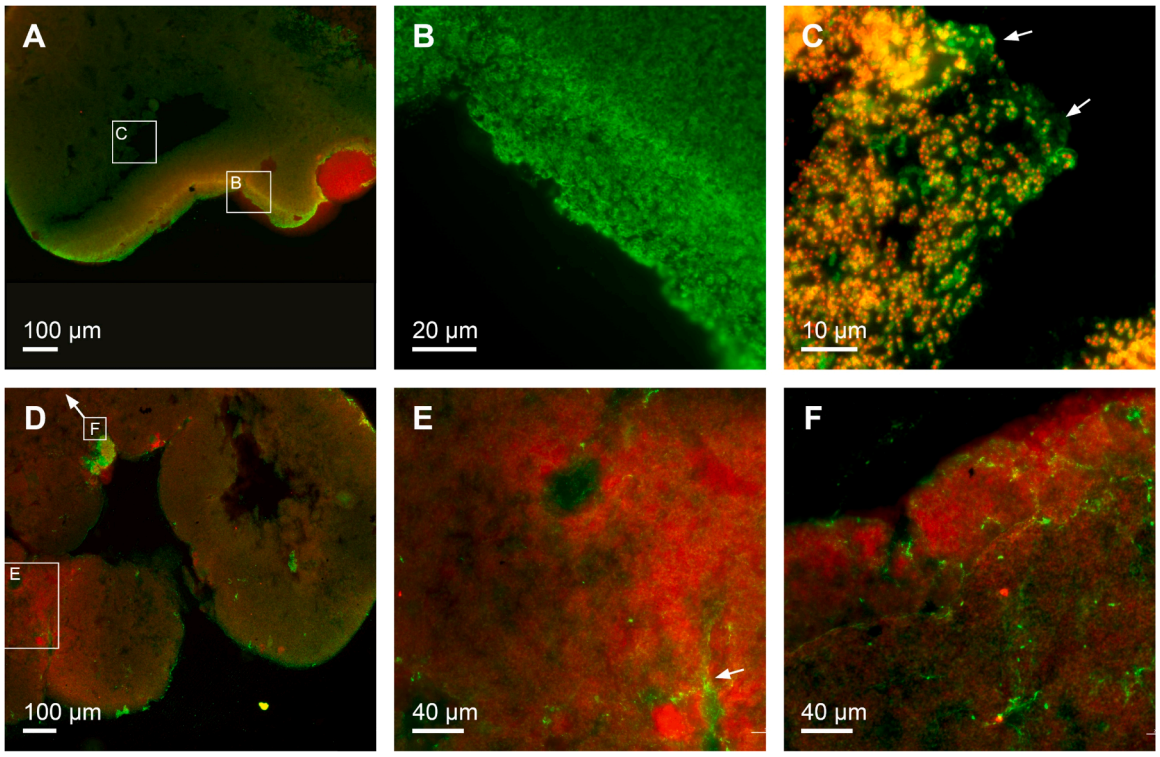

Fig. 6. Immunofluorescence staining on sliced granules. The secondary antibody probe AlexaFluor-488 (green) was overlayed with the probe for PAO651 (red). Overlap of the red and green signal results in a yellow signal. For B, only the antibody probe is shown to show the structure. C shows the surface protein surrounding the PAO651 stained "*Ca.* Accumulibacter", with the arrows indicating a web-like structure. A, B, and D show the dense honeycomb-like structure of the surface protein. E and F show the large fibre structure between the microcolonies, with the arrow in E indicate the fibre structure. A negative control without primary antibody confirmed the localized staining of the primary antibody and the autofluorescence (see Supplementary material).

on sequence level between S-layer proteins (Pum and Sleytr, 2014). The identified RTX motifs in the sequence indicate that the surface protein may belong to the family of RTX proteins that are exported by the type 1 secretion system (Linhartová et al., 2010; Sleytr et al., 2014). The physicochemical properties of the surface protein match well with known S-layers as well as RTX proteins. The hydrophobic amino acids make up 44.7 %, falling into the range of the S-layer proteins 40 – 60 %. In addition, the acidic pI of 4.3 (typical range 3.2 – 4.9) and the lack of cysteine in the amino acid sequence are characteristic of RTX proteins (Linhartová et al., 2010). Also, the predicted secondary structure matches closely to other reported S-layer proteins (Sára and Sleytr, 2000); The proportion of β-sheets, 35.2 %, is lower than the typical values of S-layer proteins of 40 % β-sheets. Whereas, the α-helix, 18.8 %, falls in the expected range (10–20 %). The α-helix arrangement at the N-terminal is also typical for S-layer proteins. Therefore, based on the similarities, the identified abundant surface protein highly resembles an S-layer RTX protein.

"*Ca.* Accumulibacter" is a known EPS-forming organism and is mainly known for its phosphate removal activity in EBPR systems. Previous works on the EPS of "*Ca.* Accumulibacter" have mainly been focused on the glycoconjugates (Chen et al., 2024; Dueholm et al., 2023; Tomás-Martínez et al., 2021). In parallel, EPS proteins are another important component to be characterized. This study suggests that there might be an S-layer Ca^{2+} binding RTX protein produced by "*Ca.* Accumulibacter" present in the EPS. In fact, one study proposed before, that Ca^{2+}-binding RTX proteins produced by different Accumulibacter species may be part of the EPS (Martín et al., 2006). However, additional FISH analysis did not conclusively identify the specific Accumulibacter species in this study (Supplementary material) and BLAST analysis on the "*Ca.* Accumulibacter" taxa did not reveal clear homology on sequence level either (Supplementary material), as expected from the S-layer proteins (Pum and Sleytr, 2014). Thus, future research should focus on which species produce this surface protein to understand how widespread the protein is and the factors influencing its production. Moreover, future research should visualize potential crystalline lattices on the "*Ca.* Accumulibacter" cell surface using electron microscopy to confirm the presence of S-layer proteins and explore their assembly and functions (Sleytr et al., 2014).

4.2. *Function of the surface protein in the EPS of seawater-adapted AGS*

The recovered surface protein has similarities with known S-layer protein. Immunostaining confirmed the location of the protein both on the cell surface and in the extracellular matrix. Similar to trehalose production and the alteration of EPS glycans (Chen et al., 2023b; de Graaff et al., 2020b), the production of the surface protein might be another response to the osmotic stress when exposed to seawater conditions in "*Ca.* Accumulibacter"-dominant AGS. It is reasonable to speculate that for the "*Ca.* Accumulibacter" cells, the surface protein might play a role in stabilizing the membrane under high osmotic pressure similar to the S-layer protein in archaea, *Lactobacillus* and *Pseudoalteromonas* (Ali et al., 2020; Engelhardt, 2007; Palomino et al., 2016). In addition, the high Ca^{2+} concentration in seawater (9.6 mM in seawater *vs.* 0.26 mM in freshwater) may facilitate the folding of the RTX motifs with Ca^{2+} on the outer membrane and in the EPS (Bumba et al., 2016). As Ca^{2+} binding is one of the structural properties of the EPS (Felz et al., 2016), the surface protein might likely be a component of the structural EPS. Overall, the abundant surface protein of "*Ca.* Accumulibacter" can be a component of the structural EPS and may function as a scaffold to stabilize its membranes under seawater conditions.

Besides on the cell surface, it was also observed that the surface protein forms a honeycomb-like structure in the microcolonies and large fibers between the microcolonies in the extracellular matrix. As S-layer

proteins are known to be shed from the cell, the interaction between the shed surface protein and other matrix components (*e.g.* metal ions, proteins, carbohydrates) may contribute to the formation of these types of structures (Ali et al., 2020; Kish et al., 2016; Wong et al., 2023). Future work employing high resolution microscopy (*i.e.* TEM, confocal microscopy) will provide more understanding of the role of the surface protein in aerobic granular sludge formation (Ali et al., 2020). Overall, this study suggests that surface proteins might not only play a role in stabilizing the cell membranes but also forming fibril structures that influence the mechanical properties of aerobic granular sludge.

It was worth noting that, S-layer proteins have been identified in the EPS of anammox granules and are thought to have a structural role within the EPS matrix (Boleij et al., 2018; Wong et al., 2023). Furthermore, one of the functions proposed in literature is their involvement in biofilm formation, *e.g.* S-layer proteins of *Tannerella forsythia* was up-regulated when grown as biofilms (Pham et al., 2010). Therefore, although there is no general function assigned to the S-layer proteins, it is reasonable to speculate that surface proteins (*e.g.* S-layer proteins) might be one of the structural proteins in granular sludge, or even in biofilm in general.

4.3. Detection of structural proteins by in-situ imaging in biofilm

EPS plays an important role in maintaining biofilm stability (Flemming and Wingender, 2010). Identifying the EPS components will allow a better understanding of the EPS functionality. Proteins are one of the major components in the EPS. In order to identify the proteins that play a structural role in EPS, a multidisciplinary approach has been proposed involving separation, and identification combined with *in situ* imaging visualization (Seviour et al., 2019). However, the steps between protein identification and *in situ* imaging by using antibodies are not clearly defined. Moreover, with the fast development of analytical techniques, recent advances in the methodology should be taken into account. Therefore, in the current research, this multidisciplinary approach was updated and expanded (Fig. 7). The same general steps as proposed in the roadmap by Seviour et al. (2019) were followed: an optimized EPS extraction on the biofilm, followed by protein separation on the SDS-PAGE and identification of the dominant protein by MS. Antibody generation with subsequent Western Blotting to evaluate specificity and finally, *in situ* imaging using immunostaining-FISH.

In practice, the following steps were identified as essential for the workflow: Optimization of the protein extraction and verification of antibodies through combined techniques. Protein extraction is a crucial step, obtaining sufficient amounts can be challenging (Boleij et al., 2019; Seviour et al., 2019). It is noted that complete solubilization of EPS can provide information regarding proteins; however, it may hinder the identification of structural proteins by compromising the clarity of the protein bands in SDS-PAGE. It is suggested in the current research that to identify proteins that play a structural role, prioritizing sufficient protein amounts to get clear bands in the SDS-PAGE is more important than achieving complete solubilization of the EPS, because it can simplify the subsequent MS analysis. Therefore, extraction conditions (*e.g.* temperature, chemical and time) have to be optimized. Moreover, protein glycosylation can interfere with SDS-PAGE separation and MS analysis (Boleij et al., 2019; Chen et al., 2023a; Gagliano et al., 2018), therefore the presence of glycoproteins should be assessed and if present, deglycosylation should be performed if possible. Furthermore, to confirm the extracellular location of the EPS protein, *in situ* verification is required. Antibody staining, known for its high specificity, is commonly used for this purpose. Typically, knock-out organisms incapable of producing the

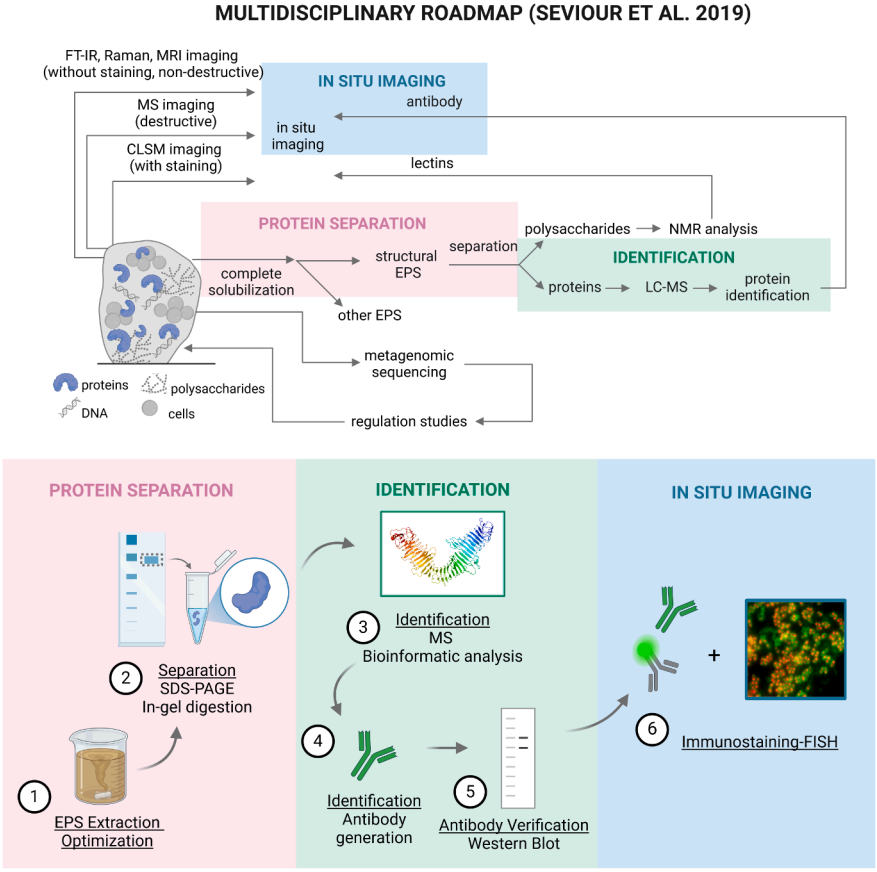

Fig. 7. General workflow to identify structural proteins in EPS put in the context of the multidisciplinary roadmap proposed by Seviour et al. (2019). The first step "complete solubilization" could be reconsidered into the optimization of EPS extraction. Microbial community analysis (FISH) should be considered in parallel to the roadmap linking with *in situ* imaging to identify the protein producer. Created in BioRender.

target protein are used as a control (Griffiths and Lucocq, 2014). However, this approach is not feasible in microbial communities, due to its complexity and dynamic interactions between community members. Thus, combining antibody staining with microbial ecology techniques, such as immunostaining-FISH and proteomic analysis, is essential to identify the producer for proper validation.

5. Conclusions

- Seawater-adapted AGS EPS contains an abundant surface protein produced by "*Ca.* Accumulibacter".
- The surface protein resembles S-layer RTX proteins and is localized both on the cell surface of "*Ca.* Accumulibacter" and in the extracellular matrix of granular sludge as large macromolecular structures.
- Detection of structural proteins in mixed-species biofilms requires optimized extraction protocols and *in situ* imaging validation using a combination of immunostaining-FISH and proteomics.

Declaration of generative AI and AI-assisted technologies in the writing process

During the preparation of this work the author(s) used ChatGPT GPT-4o in order to improve the readability and structure. After using this tool/service, the author(s) reviewed and edited the content as needed and take(s) full responsibility for the content of the publication.

CRediT authorship contribution statement

Le Min Chen: Writing – review & editing, Writing – original draft, Investigation, Data curation, Conceptualization. **Tessa Hofstra:** Investigation. **Jelle Langedijk:** Writing – review & editing, Methodology, Investigation. **Sebastian Andrei:** Writing – review & editing, Methodology. **Martin Pabst:** Writing – review & editing, Methodology, Data curation. **Mario Pronk:** Writing – review & editing, Supervision. **Mark C.M. van Loosdrecht:** Writing – review & editing, Supervision. **Yuemei Lin:** Writing – review & editing, Supervision, Investigation, Funding acquisition, Conceptualization.

Declaration of competing interest

The authors declare that they have no known competing financial interests or personal relationships that could have appeared to influence the work reported in this paper.

Acknowledgements

This research was financially supported by TKI Chemie 2017 (co-funded by Haskoning), from the Dutch Ministry of Economic Affairs and Climate Policy.

Supplementary materials

Supplementary material associated with this article can be found, in the online version, at doi:10.1016/j.watres.2025.124187.

Data availability

Data will be made available on request.

References

Abramson, J., Adler, J., Dunger, J., Evans, R., Green, T., Pritzel, A., Ronneberger, O., Willmore, L., Ballard, A.J., Bambrick, J., Bodenstein, S.W., Evans, D.A., Hung, C.-C., O'Neill, M., Reiman, D., Tunyasuvunakool, K., Wu, Z., Žemgulytė, A., Arvaniti, E., Beattie, C., Bertolli, O., Bridgland, A., Cherepanov, A., Congreve, M., Cowen-Rivers, A.I., Cowie, A., Figurnov, M., Fuchs, F.B., Gladman, H., Jain, R., Khan, Y.A., Low, C.M.R., Perlin, K., Potapenko, A., Savy, P., Singh, S., Stecula, A., Thillaisundaram, A., Tong, C., Yakneen, S., Zhong, E.D., Zielinski, M., Žídek, A., Bapst, V., Kohli, P., Jaderberg, M., Hassabis, D., Jumper, J.M., 2024. Accurate structure prediction of biomolecular interactions with AlphaFold 3. Nature 630, 493–500. https://doi.org/10.1038/s41586-024-07487-w.

Albertsen, M., McIlroy, S.J., Stokholm-Bjerregaard, M., Karst, S.M., Nielsen, P.H., 2016. Candidatus Propionivibrio aalborgensis": a novel glycogen accumulating organism abundant in full-scale enhanced biological phosphorus removal plants. Front. Microbiol. 7, 1033. https://doi.org/10.3389/FMICB.2016.01033.

Ali, S., Jenkins, B., Cheng, J., Lobb, B., Wei, X., Egan, S., Charles, T.C., McConkey, B.J., Austin, J., Doxey, A.C., 2020. Slr4, a newly identified S-layer protein from marine gammaproteobacteria, is a major biofilm matrix component. Mol. Microbiol. 114, 979–990. https://doi.org/10.1111/MMI.14588.

Amann, R.I., Binder, B.J., Olson, R.J., Chisholm, S.W., Devereux, R., Stahl, D.A., 1990. Combination of 16S rRNA-targeted oligonucleotide probes with flow cytometry for analyzing mixed microbial populations. Appl. Environ. Microbiol. 56, 1919–1925. https://doi.org/10.1128/AEM.56.6.1919-1925.1990.

APHA, 1998. Standard Methods For the Examination of Water and Wastewater, 20th ed. American Public Health Association, American Water Works Association, Water Environment Federation, Washington, D.C. 1998.

Bassin, J.P., Pronk, M., Muyzer, G., Kleerebezem, R., Dezotti, M., van Loosdrecht, M.C. M., 2011. Effect of elevated salt concentrations on the aerobic granular sludge process: linking microbial activity with microbial community structure. Appl. Environ. Microbiol. 77, 7942–7953. https://doi.org/10.1128/AEM.05016-11.

Bharat, T.A.M., Kureisaite-Ciziene, D., Hardy, G.G., Yu, E.W., Devant, J.M., Hagen, W.J. H., Brun, Y.V., Briggs, J.A.G., Löwe, J., 2017. Structure of the hexagonal surface layer on *Caulobacter crescentus* cells. Nat. Microbiol. 2. https://doi.org/10.1038/NMICROBIOL.2017.59.

Boleij, M., Pabst, M., Neu, T.R., Van Loosdrecht, M.C.M., Lin, Y., 2018. Identification of glycoproteins isolated from extracellular polymeric substances of full-scale anammox granular sludge. Environ. Sci. Technol. 52, 13127–13135. https://doi.org/10.1021/acs.est.8b03180.

Boleij, M., Seviour, T., Wong, L.L., van Loosdrecht, M.C.M., Lin, Y., 2019. Solubilization and characterization of extracellular proteins from anammox granular sludge. Water Res 164, 114952. https://doi.org/10.1016/j.watres.2019.114952.

Bumba, L., Masin, J., Macek, P., Wald, T., Motlova, L., Bibova, I., Klimova, N., Bednarova, L., Veverka, V., Kachala, M., Svergun, D.I., Barinka, C., Sebo, P., 2016. Calcium-driven folding of RTX domain β-rolls ratchets translocation of RTX proteins through type I secretion ducts. Mol. Cell 62, 47–62. https://doi.org/10.1016/J.MOLCEL.2016.03.018.

Campo, R., Corsino, S.F., Torregrossa, M., Di Bella, G., 2018. The role of extracellular polymeric substances on aerobic granulation with stepwise increase of salinity. Sep. Purif. Technol. 195, 12–20. https://doi.org/10.1016/j.seppur.2017.11.074.

Chen, L.M., Beck, P., van Ede, J., Pronk, M., van Loosdrecht, M.C.M., Lin, Y., 2024. Anionic extracellular polymeric substances extracted from seawater-adapted aerobic granular sludge. Appl. Microbiol. Biotechnol. 1081 (108), 1–12. https://doi.org/10.1007/S00253-023-12954-X, 2024.

Chen, L.M., de Bruin, S., Pronk, M., Sousa, D.Z., van Loosdrecht, M.C.M., Lin, Y., 2023a. Sialylation and sulfation of anionic glycoconjugates are common in the extracellular polymeric substances of both aerobic and Anaerobic granular sludges. Environ. Sci. Technol. 57, 13217–13225. https://doi.org/10.1021/acs.est.2c09586.

Chen, L.M., Keisham, S., Tateno, H., Ede, J.van, Pronk, M., Loosdrecht, M.C.M.van, Lin, Y., 2023b. Alterations of Glycan Composition in Aerobic Granular Sludge during the Adaptation to Seawater Conditions. ACS ES&T Water. https://doi.org/10.1021/ACSESTWATER.3C00625.

Corsino, S.F., Capodici, M., Torregrossa, M., Viviani, G., 2017. Physical properties and extracellular Polymeric substances pattern of aerobic granular sludge treating hypersaline wastewater. Bioresour. Technol. 229, 152–159. https://doi.org/10.1016/j.biortech.2017.01.024.

Crocetti, G.R., Hugenholtz, P., Bond, P.L., Schuler, A., Keller, J., Jenkins, D., Blackall, L. L., 2000. Identification of polyphosphate-accumulating organisms and design of 16S rRNA-directed probes for their detection and quantitation. Appl. Environ. Microbiol. 66, 1175–1182. https://doi.org/10.1128/AEM.66.3.1175-1182.2000.

Daims, H., Brühl, A., Amann, R., Schleifer, K.H., Wagner, M., 1999. The domain-specific probe EUB338 is insufficient for the detection of all bacteria: development and evaluation of a more comprehensive probe set. Syst. Appl. Microbiol. 22, 434–444. https://doi.org/10.1016/S0723-2020(99)80053-8.

de Graaff, D.R., Felz, S., Neu, T.R., Pronk, M., van Loosdrecht, M.C.M., Lin, Y., 2019. Sialic acids in the extracellular polymeric substances of seawater-adapted aerobic granular sludge. Water Res 343–351. https://doi.org/10.1016/j.watres.2019.02.040.

de Graaff, D.R., van Loosdrecht, M.C.M., Pronk, M., 2020a. Biological phosphorus removal in seawater-adapted aerobic granular sludge. Water Res 172, 115531. https://doi.org/10.1016/J.WATRES.2020.115531.

de Graaff, D.R., van Loosdrecht, M.C.M., Pronk, M., 2020b. Trehalose as an osmolyte in Candidatus Accumulibacter phosphatis. Appl. Microbiol. Biotechnol. 1051 (105), 379–388. https://doi.org/10.1007/S00253-020-10947-8, 2020.

Decho, A.W., Gutierrez, T., 2017. Microbial extracellular polymeric substances (EPSs) in ocean systems. Front. Microbiol. 8, 922. https://doi.org/10.3389/fmicb.2017.00922.

Dueholm, M.K.D., Besteman, M., Zeuner, E.J., Riisgaard-Jensen, M., Nielsen, M.E., Vestergaard, S.Z., Heidelbach, S., Bekker, N.S., Nielsen, P.H., 2023. Genetic potential for exopolysaccharide synthesis in activated sludge bacteria uncovered by genome-resolved metagenomics. Water Res 229, 119485. https://doi.org/10.1016/J.WATRES.2022.119485.

Dunker, A.K., Rueckert, R.R., 1969. Observations on molecular weight determinations on polyacrylamide gel. J. Biol. Chem. 244. https://doi.org/10.1016/s0021-9258(18)94310-3.

Elahinik, A., Li, L., Pabst, M., Abbas, B., Xevgenos, D., van Loosdrecht, M.C.M., Pronk, M., 2023. Aerobic granular sludge phosphate removal using glucose. Water Res 247, 120776. https://doi.org/10.1016/J.WATRES.2023.120776.

Engelhardt, H., 2007. Mechanism of osmoprotection by archaeal S-layers: a theoretical study. J. Struct. Biol. 160, 190–199. https://doi.org/10.1016/J.JSB.2007.08.004.

Felz, S., Al-Zuhairy, S., Aarstad, O.A., van Loosdrecht, M.C.M., Lin, Y.M., 2016. Extraction of structural extracellular polymeric substances from aerobic granular sludge. J. Vis. Exp. 54534. https://doi.org/10.3791/54534, 2016.

Flemming, H.C., Wingender, J., 2010. The biofilm matrix. Nat. Rev. Microbiol. https://doi.org/10.1038/nrmicro2415.

Gagliano, M.C., Neu, T.R., Kuhlicke, U., Sudmalis, D., Temmink, H., Plugge, C.M., 2018. EPS glycoconjugate profiles shift as adaptive response in anaerobic microbial granulation at high salinity. Front. Microbiol. 9, 1423. https://doi.org/10.3389/fmicb.2018.01423.

Griffiths, G., Lucocq, J.M., 2014. Antibodies for immunolabeling by light and electron microscopy: not for the faint hearted. Histochem. Cell Biol. 142, 347. https://doi.org/10.1007/S00418-014-1263-5.

Guo, S., Vance, T.D.R., Stevens, C.A., Voets, I., Davies, P.L., 2019. RTX adhesins are key bacterial surface megaproteins in the formation of biofilms. Trends Microbiol 27, 453–467. https://doi.org/10.1016/J.TIM.2018.12.003.

Kim, J.S., Song, S., Lee, M., Lee, S., Lee, K., Ha, N.C., 2016. Crystal structure of a soluble fragment of the membrane fusion protein HlyD in a type i secretion system of gram-negative bacteria. Structure 24, 477–485. https://doi.org/10.1016/j.str.2015.12.012.

Kish, A., Miot, J., Lombard, C., Guigner, J.M., Bernard, S., Zirah, S., Guyot, F., 2016. Preservation of archaeal surface layer structure during mineralization. Sci. Reports 61 (6), 1–10. https://doi.org/10.1038/srep26152, 2016.

Kleikamp, H.B.C., Pronk, M., Tugui, C., Guedes da Silva, L., Abbas, B., Lin, Y.M., van Loosdrecht, M.C.M., Pabst, M., 2021. Database-independent de novo metaproteomics of complex microbial communities. Cell Syst 12, 375–383. https://doi.org/10.1016/J.CELS.2021.04.003 e5.

Lefebvre, O., Moletta, R., 2006. Treatment of organic pollution in industrial saline wastewater: a literature review. Water Res. https://doi.org/10.1016/j.watres.2006.08.027.

Lin, Y., Reino, C., Carrera, J., Pérez, J., van Loosdrecht, M.C.M., 2018. Glycosylated amyloid-like proteins in the structural extracellular polymers of aerobic granular sludge enriched with ammonium-oxidizing bacteria. Microbiologyopen 7, e00616. https://doi.org/10.1002/mbo3.616.

Linhartová, I., Bumba, L., Mašn, J., Basler, M., Osička, R., Kamanová, J., Procházková, K., Adkins, I., HejnováHolubová, J., Sadílková, L., Morová, J., Šebo, P., 2010. RTX proteins: a highly diverse family secreted by a common mechanism. Fems Microbiol. Rev. 34, 1076. https://doi.org/10.1111/J.1574-6976.2010.00231.X.

Martín, H.G., Ivanova, N., Kunin, V., Warnecke, F., Barry, K.W., McHardy, A.C., Yeates, C., He, S., Salamov, A.A., Szeto, E., Dalin, E., Putnam, N.H., Shapiro, H.J., Pangilinan, J.L., Rigoutsos, I., Kyrpides, N.C., Blackall, L.L., McMahon, K.D., Hugenholtz, P., 2006. Metagenomic analysis of two enhanced biological phosphorus removal (EBPR) sludge communities. Nat. Biotechnol. 24, 1263–1269. https://doi.org/10.1038/nbt1247.

McSwain, B.S., Irvine, R.L., Hausner, M., Wilderer, P.A., 2005. Composition and distribution of extracellular polymeric substances in aerobic flocs and granular sludge. Appl. Environ. Microbiol. 71, 1051–1057. https://doi.org/10.1128/AEM.71.2.1051-1057.2005.

Ou, D., Li, W., Li, H., Wu, X., Li, C., Zhuge, Y., Liu, Y.di, 2018. Enhancement of the removal and settling performance for aerobic granular sludge under hypersaline stress. Chemosphere 212, 400–407. https://doi.org/10.1016/J.CHEMOSPHERE.2018.08.096.

Pabst, M., Grouzdev, D.S., Lawson, C.E., Kleikamp, H.B.C., de Ram, C., Louwen, R., Lin, Y.M., Lücker, S., van Loosdrecht, M.C.M., Laureni, M., 2022. A general approach to explore prokaryotic protein glycosylation reveals the unique surface layer modulation of an anammox bacterium. ISME J 16, 346–357. https://doi.org/10.1038/S41396-021-01073-Y.

Palomino, M.M., Waehner, P.M., Fina Martin, J., Ojeda, P., Malone, L., Sánchez Rivas, C., Prado Acosta, M., Allievi, M.C., Ruzal, S.M., 2016. Influence of osmotic stress on the profile and gene expression of surface layer proteins in *Lactobacillus acidophilus* ATCC 4356. Appl. Microbiol. Biotechnol. 100, 8475–8484. https://doi.org/10.1007/S00253-016-7698-Y/FIGURES/4.

Pearson, W.R., 2013. An introduction to sequence similarity ("homology") searching. Curr. Protoc. Bioinforma. 3. https://doi.org/10.1002/0471250953.bi0301s42, 0.

Pham, T.K., Roy, S., Noirel, J., Douglas, I., Wright, P.C., Stafford, G.P., 2010. A quantitative proteomic analysis of biofilm adaptation by the periodontal pathogen Tannerella forsythia. Proteomics 10, 3130–3141. https://doi.org/10.1002/PMIC.200900448;SUBPAGE:STRING:FULL.

Pronk, M., de Kreuk, M.K., de Bruin, B., Kamminga, P., Kleerebezem, R., van Loosdrecht, M.C.M., 2015. Full scale performance of the aerobic granular sludge process for sewage treatment. Water Res 84, 207–217. https://doi.org/10.1016/j.watres.2015.07.011.

Pum, D., Sleytr, U.B., 2014. Reassembly of S-layer proteins. Nanotechnology 25, 312001. https://doi.org/10.1088/0957-4484/25/31/312001.

Sára, M., Sleytr, U.B., 2000. S-layer proteins. J. Bacteriol. 182, 859. https://doi.org/10.1128/JB.182.4.859-868.2000.

Scheller, C., Krebs, F., Wiesner, R., Wätzig, H., Oltmann-Norden, I., 2021. A comparative study of CE-SDS, SDS-PAGE, and Simple Western—Precision, repeatability, and apparent molecular mass shifts by glycosylation. Electrophoresis 42, 1521–1531. https://doi.org/10.1002/ELPS.202100068.

Seviour, T., Derlon, N., Dueholm, M.S., Flemming, H.-C., Girbal-Neuhauser, E., Horn, H., Kjelleberg, S., van Loosdrecht, M.C.M., Lotti, T., Malpei, M.F., Nerenberg, R., Neu, T. R., Paul, E., Yu, H., Lin, Y., 2019. Extracellular polymeric substances of biofilms: suffering from an identity crisis. Water Res 151, 1–7. https://doi.org/10.1016/j.watres.2018.11.020.

Sleytr, U.B., Schuster, B., Egelseer, E.M., Pum, D., 2014. S-layers: principles and applications. FEMS Microbiol. Rev. 38, 823–864. https://doi.org/10.1111/1574-6976.12063.

Spitz, O., Erenburg, I.N., Beer, T., Kanonenberg, K., Holland, I.B., Schmitt, L., 2019. Type I secretion systems—One mechanism for all? Microbiol. Spectr. 7. https://doi.org/10.1128/MICROBIOLSPEC.PSIB-0003-2018/ASSET/9C2920A1-D783-4A4A-93C7-5819E4025BCB/ASSETS/GRAPHIC/PSIB-0003-2018-FIG3.GIF.

Teufel, F., Almagro Armenteros, J.J., Johansen, A.R., Gíslason, M.H., Pihl, S.I., Tsirigos, K.D., Winther, O., Brunak, S., von Heijne, G., Nielsen, H., 2022. SignalP 6.0 predicts all five types of signal peptides using protein language models. Nat. Biotechnol. 40, 1023–1025. https://doi.org/10.1038/S41587-021-01156-3.

Tomás-Martínez, S., Kleikamp, H.B.C., Neu, T.R., Pabst, M., Weissbrodt, D.G., van Loosdrecht, M.C.M., Lin, Y., 2021. Production of nonulosonic acids in the extracellular polymeric substances of "Candidatus Accumulibacter phosphatis. Appl. Microbiol. Biotechnol. 105, 3327–3338. https://doi.org/10.1007/s00253-021-11249-3.

Van Loosdrecht, M.C.M., Brdjanovic, D., 2014. Anticipating the next century of wastewater treatment. Science (80-.) 344, 1452–1453. https://doi.org/10.1126/SCIENCE.1255183/ASSET/4AFA3CFE-23CA-4751-8D4F-94D23DF70A18/ASSETS/GRAPHIC/344_1452_F2.JPEG.

Weissbrodt, D.G., Shani, N., Holliger, C., 2014. Linking bacterial population dynamics and nutrient removal in the granular sludge biofilm ecosystem engineered for wastewater treatment. FEMS Microbiol. Ecol. 88, 579–595. https://doi.org/10.1111/1574-6941.12326.

Welles, L., Tian, W.D., Saad, S., Abbas, B., Lopez-Vazquez, C.M., Hooijmans, C.M., van Loosdrecht, M.C.M., Brdjanovic, D., 2015. Accumulibacter clades type I and II performing kinetically different glycogen-accumulating organisms metabolisms for anaerobic substrate uptake. Water Res 83, 354–366. https://doi.org/10.1016/j.watres.2015.06.045.

Wong, L.L., Lu, Y., Ho, J.C.S., Mugunthan, S., Law, Y., Conway, P., Kjelleberg, S., Seviour, T., 2023. Surface-layer protein is a public-good matrix exopolymer for microbial community organisation in environmental anammox biofilms. ISME J. 176 (17), 803–812. https://doi.org/10.1038/s41396-023-01388-y, 2023.

Zhang, Z., Liu, J., Xiao, C., Chen, G., 2023a. Making waves: enhancing sustainability and resilience in coastal cities through the incorporation of seawater into urban metabolism. Water Res 242, 120140.

Zhang, Z., Sato, Y., Dai, J., Chui, H.kwong, Daigger, G., Van Loosdrecht, M.C.M., Chen, G., 2023b. Flushing toilets and cooling spaces with seawater improve water–energy securities and achieve carbon mitigations in coastal cities. Environ. Sci. Technol. 57, 5068–5078.

Zhao, Y., Zhuang, X., Ahmad, S., Sung, S., Ni, S.Q., 2020a. Biotreatment of high-salinity wastewater: current methods and future directions. World J. Microbiol. Biotechnol. https://doi.org/10.1007/s11274-020-02815-4.

Zhao, Y., Zhuang, X., Ahmad, S., Sung, S., Ni, S.Q., 2020b. Biotreatment of high-salinity wastewater: current methods and future directions. World J. Microbiol. Biotechnol. 36, 1–11. https://doi.org/10.1007/S11274-020-02815-4/TABLES/2.

Zhu, L., Zhou, J., Lv, M., Yu, H., Zhao, H., Xu, X., 2015. Specific component comparison of extracellular polymeric substances (EPS) in flocs and granular sludge using EEM and SDS-PAGE. Chemosphere 121, 26–32. https://doi.org/10.1016/J.CHEMOSPHERE.2014.10.053.